Radiative proton capture to excited states in ^{16}O

J. D. Kalen, H. J. Hausman, A. Abduljalil, W. Kim,* D. G. Marchlenski, J. P. McDermott, and T. W. Rackers†
Department of Physics, Ohio State University, Columbus, Ohio 43210

S. L. Blatt‡
Department of Physics, Ohio State University, Columbus, Ohio 43210 and Department of Physics, Clark University, Worcester, Massachusetts 01610

M. A. Kovash
Department of Physics, University of Kentucky, Lexington, Kentucky 40506

A. D. Bacher
Department of Physics, Indiana University, Bloomington, Indiana 47401
(Received 30 June 1988)

The radiative proton capture reaction on ^{15}N was measured over the energy region $E_p = 20$–90 MeV. Presented are experimental differential cross sections at $\theta_\gamma = 60°$ for captures populating the ground and various excited states of ^{16}O. Differential cross sections and analyzing-power angular distributions are presented at a proton energy of $E_p = 49.69$ MeV. Calculations from a phenomenological direct-semidirect and a more detailed relativistic model describe cross sections well, but are less satisfactory in describing analyzing powers. Results of the energy-dependence measurements show that there are giant resonances built on all the excited states investigated.

I. INTRODUCTION

Theories describing radiative proton capture reactions in the energy region 20 MeV $\leq E_p \leq$ 100 MeV are generally based on shell-model structure. These theories simplify for the doubly magic nucleus ^{16}O. We report here on measurements which these theories should be able to address. The $^{15}N(p,\gamma)^{16}O$ reaction was performed with a NaI(Tl) spectrometer[1] at the Indiana University Cyclotron Facility (IUCF) utilizing the pulsed, polarized proton beam. Discrimination between the neutron background and the high-energy γ rays of interest was accomplished by time-of-flight techniques; fast electronics were also employed for cosmic-ray rejection and pulse pileup reduction. With this apparatus, proton captures populating not only low-lying states, but also highly excited states in the residual nucleus, were observed. It is the purpose of this paper to provide new energy-dependent data on several excited states in ^{16}O, and some analyzing-power angular distributions which should provide a more rigorous test than cross-section angular distributions alone for differing theoretical treatments of capture reactions.

In earlier work,[2] our group reported on the existence of a giant resonance built on the cluster of final states in ^{12}C at an excitation of $\sim$19 MeV. Following this work, Anghinolfi *et al.*[32] reported the observation of giant resonances built on many of the excited states of ^{12}C; the University of Washington/Brookhaven National Laboratory collaboration[4] reported similar results in ^{28}Si. In this paper we show evidence verifying this phenomenon for the excited states of ^{16}O.

The experimental results are compared with relativistic and nonrelativistic models of the direct-semidirect (DSD) theory, both of which use 1p-1h shell-model configurations. Over a large energy region, the radiative proton capture reactions reported here can be described reasonably well using either of these theories. On the other hand, the analyzing power data indicate that further theoretical work is required.

II. EXPERIMENTAL DESCRIPTION

The $^{15}N(p,\gamma)^{16}O$ experiments were performed using the Ohio State University Medium Energy Gamma Assembly NaI(Tl) spectrometer,[1] located in the gamma cave (low-background room) at the Indiana University Cyclotron Facility. The NaI(Tl) crystal, 25 cm in diameter by 30 cm long, has seven RCA 8575 phototubes located in a hexagonal array on one end. The phototube bases are voltage regulated using an active transistor circuit. The crystal is surrounded by a plastic scintillator shield used in anticoincidence, which serves to reject cosmic rays and improve the monoenergetic gamma-ray response shape. Further details of the system are described in Ref. 5. The spectrometer was positioned 1 m from the target and subtended a solid angle of 9.16 msr. The spectrometer's energy resolution was approximately 2.2% FWHM at $E_\gamma = 40$ MeV.

The ^{15}N gas, analyzed as $>99\%$ isotopically enriched, was contained in a target cell which consisted of a hollow brass cylinder, 2.41 cm long and 1.91 cm in outside diameter, with a wall thickness of 0.081 cm. Havar foils (6.35×10^{-4} cm) were epoxied to the ends of the brass

cylinder for windows. The gas cell was typically pressurized to 2.9 atm for a total thickness of 8.8 mg/cm^2.

Raw spectra [see an example in Fig. 1(a)] included gamma rays from the entrance and exit HAVAR foils. To determine these contributions in the total spectrum, we performed runs with the gas cell completely evacuated. Spectra of the gamma rays from foils only (dashed line) showed no resolvable structure and a monotonically decreasing intensity with increasing gamma-ray energy. The empty gas cell runs were normalized to gas-filled runs by charge integration and their contributions were subtracted channel by channel from the gas-filled spectra (solid line). Typical HAVAR-foil-subtracted γ-ray spectra from the $^{15}N(p,\gamma)^{16}O$ reaction at proton energies $E_p=21.8$ and 44.5 MeV at a γ-ray angle of 60° are shown in Figs. 1(b) and (c), respectively, along with their fitted states. Table I lists the observed states of interest in ^{16}O.

The NaI(Tl) spectrometer response function to monoenergetic gamma rays is approximated by a Gaussian peak matched to a decaying exponential tail on the low-energy side; this tail is assumed to approach a constant value towards zero energy. This shape is used to fit the components of the spectra. The areas so determined are then corrected for pulse pileup and by a "resum" factor to account for events removed by the anticoincidence condition. Because of insufficient resolution of the NaI(Tl) spectrometer, gamma rays from proton captures

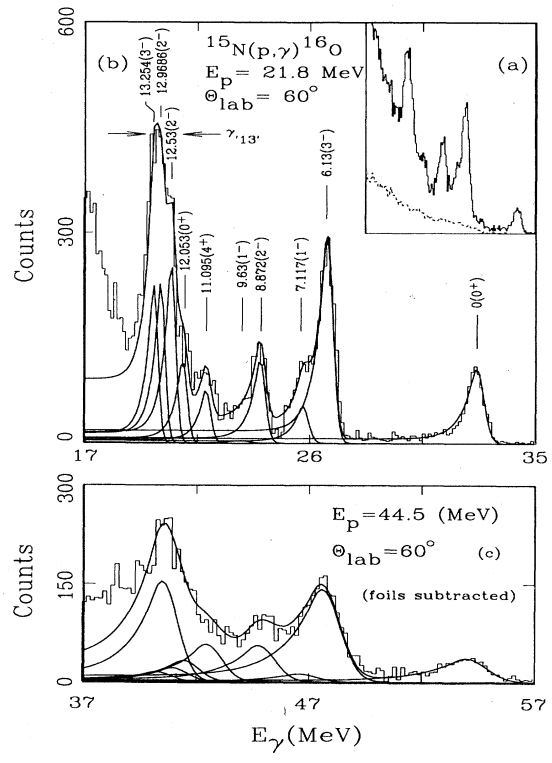

FIG. 1. Gamma-ray spectra for $^{15}N(p,\gamma)^{16}O$ at 60°, $E_p=21.8$ and 44.5 MeV. Curve (a) includes the spectra due to the ^{15}N gas and the HAVAR foils (solid line) and that due to the HAVAR foils only (dashed line). Curves (b and c) are the resultant fitted γ-ray spectrum after subtracting the foil contribution.

TABLE I. Fitted states of interest in ^{16}O (Ref. 36).

Designation	$J^\pi;T$	E_x (MeV)
γ_0	$0^+;0$	0
γ_2	$3^-;0$	6.13
γ_5	$2^-;0$	8.87
γ_6	$1^-;0$	9.63
	$2^-;0$	12.53
γ_{13}	$2^-;1$	12.97
	$3^-;1$	13.25

to the excited states near 13 MeV, labeled "γ_{13}," are treated as a composite of three inadequately resolved states: $E_x=12.53$ MeV ($J^\pi=2^-$), $E_x=12.9686$ MeV ($J^\pi=2^-$), and $E_x=13.254$ MeV ($J^\pi=3^-$). The same situation is true for the cross-section calculations of "$\gamma_{5,6}$," transitions to the unresolved states at $E_x=8.872$ MeV ($J^\pi=2^-$) and $E_x=9.632$ MeV ($J^\pi=1^-$).

The cyclotron was operated in the fast spin-flip mode, with procedures as described in Ref. 5. A monitor polarimeter, located between the injector and main cyclotron stages, contained a ^4He gas cell which could be moved into and out of the proton beam under the command of the cyclotron control system. From the pulse-height spectrum accumulated by solid-state detectors located to the left and right of the beam line, the yield of the proton elastic-scattering peaks above background were calculated. Beam polarization is defined by

$$P=\frac{1}{A_{y,p}}\frac{A_L-A_R}{A_L+A_R}, \tag{1}$$

where $A_{y,p}$ is the analyzing power for the ^4He $(\vec{p},p)^4He$ reaction, and A_L and A_R are the respective areas of the elastic-scattering peaks for the left and right solid-state detectors. The beam polarization was measured after every few runs and typically had a value of 0.70–0.74. Analyzing powers were then calculated with the gamma-ray detector on the right-hand side of the beam line using the Basel convention.

Cross sections were measured from $E_p=20$ to 90 MeV at $\theta_\gamma=60°$, and $\sigma(\theta)$ and $A_y(\theta)$ were measured for angles between 30° and 120° at $E_p=49.69$ MeV. These results are presented in Figs. 2–5.

Details of the results will be discussed after a short description of the theoretical calculations we are presenting for initial comparison with the data.

III. MODEL CALCULATIONS

A. Phenomenological direct-semidirect (DSD) calculation

The DSD reaction model for describing radiative capture of fast nucleons, first proposed by Brown[6] and modified by Lushnikov and Zaretsky,[7] by Clement, Lane, and Rook,[8] and by Potokar *et al.*[9,10] has had success in fitting (p,γ) and (n,γ) capture cross sections, particularly in the region of the giant dipole resonance (GDR). The cross section for radiative capture of a fast nucleon from the initial state into the bound single-particle state of the

final nucleus can be written as

$$\sigma^{\mathrm{DSD}}_{l'j';nlj} = \sigma^{d}_{l'j';nlj} |F_{\mathrm{eff}}(l'j';nlj)|^2 C^2S \ , \quad (2)$$

where σ^d is the direct capture cross section (Ref. 2), $l'j'$ are the initial state quantum numbers, nlj are the final state quantum numbers, F_{eff} is an effective charge factor, and C^2S is the conventional spectroscopic factor. In this work, the effective charge factor contains the form factor for $E1$ transitions, and was chosen to have a volume shape

$$h(r) \propto V_1 r f(r) \ , \quad (3)$$

where V_1 is the real part of the symmetry term in the optical potential and $f(r)$ is of the Woods-Saxon form.

Equation (2) is programmed in the computer code HIKARI,[11] which has been used previously to perform, among others, the DSD model calculations for polarized neutron capture on ^{13}C (Ref. 12) and the analysis of (p,γ) reactions previously reported by our group.[5] The present calculations include direct $E1$ and $E2$ and semidirect $E1$ strength from the isovector GDR. Semidirect $E2$ and $E3$ and direct $E3$ strength were not included due to their small contributions.[13–16] The position and width of the ground-state GDR were obtained from the literature and used as input into HIKARI. The single particle-hole configurations and the spectroscopic factors for the states of interest were obtained from (^{3}He,d) stripping reactions as reported in the literature, and are tabulated in Table II. The global optical-model parameters (OMP's) obtained from Watson, Singh, and Segal[17] for the proton energy region 10–50 MeV were used to calculate the radial wave functions of the captured particle as well as the continuum-state radial function for the incident proton. Extending these parameters to higher proton energies was discussed in our previous paper.[5] Briefly, extending these optical model parameters of Watson *et al.*,[17] as shown in our previous paper,[5] produced cross sections in the order of a magnitude greater than the experimental results for proton energies greater than 50 MeV.

B. Relativistic DSD model calculations

The relativistic shell-model calculations were performed using a program developed by one of us (J. P. McD.) which also employs both the direct and semidirect processes, but allows transitions via both single-particle and meson-exchange mechanisms. The model uses four-component Dirac wave functions. Bound-state wave functions are derived from the relativistic Hartree method of Horowitz and Serot.[18] We derive continuum wave functions using optical potentials generated by a relativistic impulse approximation (RIA) in the program DREX.[19] The RIA is used since phenomenological relativistic optical potentials[20] are not currently available for this target and energy region. Considering the sensitivity of these calculations to the initial state interaction, we consider the use of a RIA at these energies a major weakness of the calculations.

The direct process (detailed in Ref. 21) has no free parameters. In the semidirect process, the position and width of the giant dipole resonance are taken to be the same as used in HIKARI. A single scaling factor was used for the semidirect contribution to give the correct strength at the peak of the resonance. This relativistic model was programmed in the computer code GAMMA (Ref. 21) and was used to perform the radiative capture analyses reported previously.[5]

TABLE II. Spectroscopic factor and 1p-1h configuration (Ref. 29).

E_x (MeV)	1p-1h configuration	S_{lj} spectroscopic factor
0.0	$(1p_{1/2}, 1p_{1/2}^{-1})$	3.50
6.1304	$(1d_{5/2}, 1p_{1/2}^{-1})$	0.63
8.872	$(1d_{5/2}, 1p_{1/2}^{-1})$	0.55
9.632	unknown	unknown
12.53	$(1d_{3/2}, 1p_{1/2}^{-1})$	1.45
12.9686	$(1d_{5/2}, 1p_{1/2}^{-1})$	0.85
13.254	$(1d_{5/2}, 1p_{1/2}^{-1})$	0.96

IV. RESULTS

A. ^{15}N$(p,\gamma_0)^{16}$O

The energy dependence of the ^{15}N$(p,\gamma_0)^{16}$O differential cross sections at a detector angle of 60° has been reported earlier[5] and is shown in Fig. 2(a). It is included here to allow comparison with captures populating the ^{16}O excited states. Using detailed balance, the data in the vicinity of the GDR centered at $E_p = 11.0$ MeV from the ^{16}O$(\gamma,p_0)^{15}$N reaction reported by Baglin and Thompson[22] are also plotted, as are the cross sections from the ^{16}O$(\gamma,p_0)^{15}$N reaction reported by Findlay and Owens[23] at $E_\gamma = 60$, 80, and 100 MeV.

The width and position of the giant dipole resonance ($E_\gamma = 22.441$ MeV, $\Gamma_\gamma = 3.0$ MeV)[24] is input into GAMMA and HIKARI. Table III tabulates the width, position, and the energy-weighted sum rule (EWSR) of the GDR for all of the states of interest in ^{16}O.

The angular distributions of the differential cross sections and analyzing powers at a proton energy 49.69 MeV are plotted in Figs. 2(b) and (c), respectively. Using detailed balance on the ^{16}O$(\gamma,p_0)^{15}$N data[23] at a gamma-ray energy $E_\gamma = 60$ MeV allows us to also plot that angular distribution in Fig. 2(b), for comparison. Since the ^{15}N$(p,\gamma_0)^{16}$O reaction at $E_p = 49.69$ MeV produces gamma rays in the energy region 59.5 MeV $\geq E_\gamma \geq$ 57.9 MeV for angles $30° \leq \theta_{\mathrm{lab}} \leq 120°$, the comparisons should not be far off. The analyzing-power angular distribution, Fig. 2(c), shows calculations from HIKARI (dashed) and GAMMA (solid).

B. ^{15}N$(p,\gamma_2)^{16}$O

The energy dependence of the cross sections at $\theta_{\mathrm{lab}} = 60°$ is shown in Fig. 3(a). The data in the region of the GDR centered at $E_p = 16.0$ MeV were obtained from the ^{15}N$(p,\gamma_2)^{16}$O reaction reported by Chew, Low, Nelson.[25] The first excited state ($E_x = 6.05$ MeV, $J^\pi = 0^+$) was not included in these fits since the $p + ^{15}$N reaction

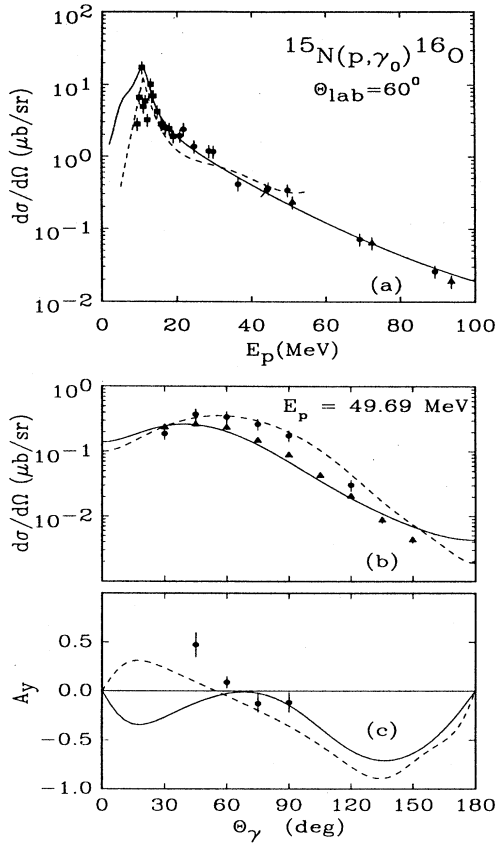

FIG. 2. Results for ground-state capture. The energy dependence of the 60° differential cross section is shown in (a). The differential cross-section and analyzing-power angular distributions at 49.69 MeV are shown in (b) and (c), respectively. The dashed curves are from the phenomenological DSD model calculations of Ref. 12. The solid curves are from the relativistic model calculations of Ref. 21. The square data points are from Ref. 22 and the triangular data points from Ref. 23, transformed by use of detailed balance.

channel strongly populates primarily 1p-1h states, while this state is predominantly 4p-4h; states that decay to it must be 3p-3h, 4p-4h, or 5p-5h.[25] Recently, Balamuth *et al.*[26] reported on the properties of the $E1$ giant resonance built upon the 0^+ first-excited state. Above the region of the GDR, the population of this state was only $\sim\frac{1}{20}$ that of the 3^- second-excited state.

The position and width of the $E1$ giant dipole resonance used in the theoretical calculations are E_γ=20.998 MeV, Γ_γ=2.75 MeV, obtained from the ^{15}N$(p,\gamma_2)^{16}$O analysis performed by Anghinolfi *et al.*[3] The γ_2 cross sections from the data by Anghinolfi *et al.*,[3] were not plotted due to the seriously different absolute values resulting from that group's data analysis method. Their assumed response function[27,28] does not include a low-energy tail which extends to zero energy, as used by our group. Not including the low-energy tail lowers their cross section relative to other mutually consistent analyses[2,4] by 20–30 %, which is approximately the area under the low-energy tail.

TABLE III. Giant dipole resonance parameters.

Designation	Position E_γ (MeV)	Width Γ (MeV)	EWSR
γ_0	22.441	3.00	0.90
γ_2	20.998	2.75	0.90
$\gamma_{5,6}$	24.818	3.75	0.80
$\gamma_{\text{"13"}}$	20.691	3.00	0.85

The angular distribution of the cross sections and the analyzing-power angular distribution at 49.69 MeV are plotted in Figs. 3(b) and (c), respectively. The analyzing-power angular distribution shows HIKARI reproducing the data more closely than GAMMA.

C. ^{15}N$(p,\gamma_{5,6})^{16}$O

The cross section as a function of energy is plotted in Fig. 4(a). The fifth-excited state, E_x=8.872 MeV ($J^\pi=2^-$), is the dominant state of this group with a $(1d_{5/2}, 1p_{1/2}^{-1})$ configuration as determined by the ^{15}N$(^3$He,$d)^{16}$O reaction.[29] No stripping reaction data were available for the sixth-excited state, E_x=9.632 MeV ($J^\pi=1^-$). Due to the dominance of the fifth-excited

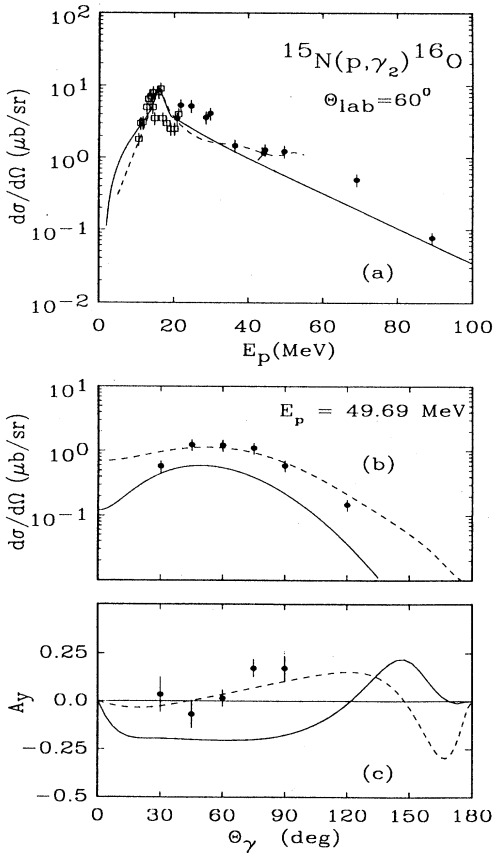

FIG. 3. Same as Fig. 2, for capture to the ^{16}O second-excited state. The square data points are from Ref. 25.

state as shown in Fig. 1, and no information on significant particle-hole components in the sixth-excited state, only the fifth-excited state was used in the theoretical comparisons. Summing the areas of the unresolved states γ_5 and γ_6, the experimental cross sections and analyzing powers were determined. The position and width of the GDR, $E_\gamma = 24.818$ MeV, $\Gamma_\gamma = 3.75$ MeV, were determined by optimization of the fits to our data.

The angular distributions of the cross sections and the analyzing powers are shown in Figs. 4(b) and (c), respectively.

D. $^{15}N(p,\gamma_{\text{"13"}})^{16}O$

The cluster of states at an excitation energy of approximately 13 MeV in ^{16}O is composed of at least three unresolved states. As Dowell *et al.* have shown,[4] the 1p-1h states most strongly excited in (p,γ) capture are the same states excited in $(^3He,d)$ transfer reactions. From the $^{15}N(^3He,d)^{16}O$ results of Fulbright *et al.*,[29] the states strongly excited at excitation energies near 13 MeV in ^{16}O are the $E_x = 12.53$ MeV ($J^\pi = 2^-$), $E_x = 12.97$ MeV ($J^\pi = 2^-$), and $E_x = 13.25$ MeV ($J^\pi = 3^-$) states. By assuming these three states were the dominant components of the $\gamma_{\text{"13"}}$ cluster, reasonable fits to the (p,γ) spectra were obtained at all angles. The spectroscopic factors reported in Ref. 29 were then used in both HIKARI and GAMMA calculations for this cluster as well as for the other states investigated.

Neither of the models used was capable of calculating cross sections and analyzing powers populating unbound states such as the $\gamma_{\text{"13"}}$ cluster. In order to obtain cross sections and analyzing powers for these unbound states, we assumed a small binding energy of 5 keV for the calculations. It is not clear how seriously this affects the validity of the calculations. However, we found that the differential cross sections calculated by the program HIKARI under these conditions had the proper shape for the angular distribution and resulted in an absolute cross section only 8% larger than the data.

The energy dependence of the cross section at $\theta_{lab} = 60°$ is shown in Fig. 5(a), for the complete $\gamma_{\text{"13"}}$ structure. The theoretical differential cross sections for the cluster were obtained by calculating the cross sections for the three members of the cluster, using the parameters of Tables I, II, and III, and then adding their cross sections. The theoretical HIKARI calculations were all normalized

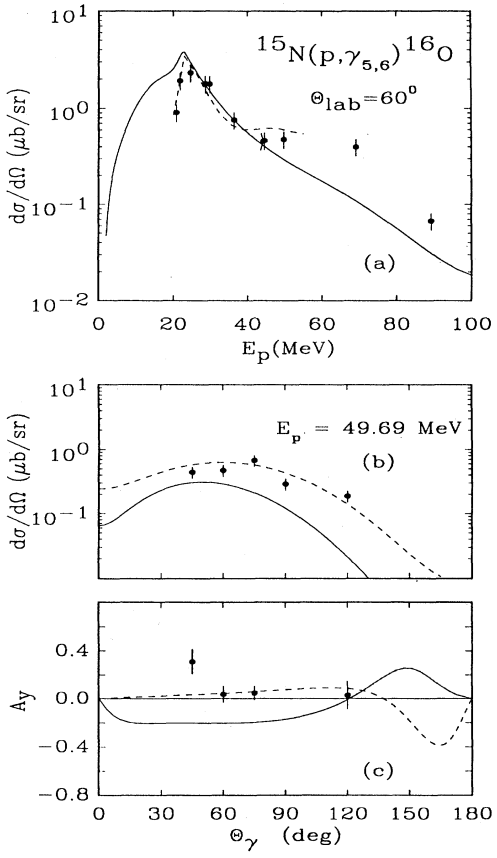

FIG. 4. Same as Fig. 2, for captures to the fifth- and sixth-excited states.

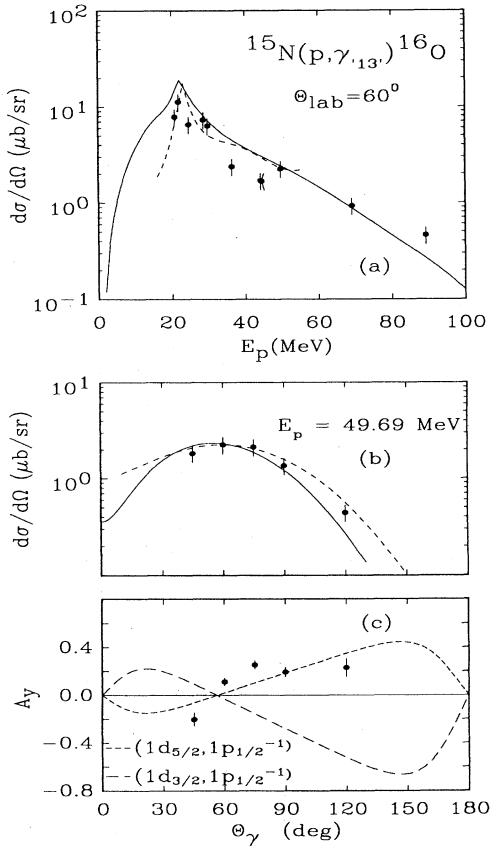

FIG. 5. Same as Fig. 2, for captures to the states near 13 MeV excitation. The analyzing-power angular distribution (c) shows possible single particle-hole contributions using the phenomenological DSD calculation HIKARI. The long- and short-dash curves represents pure 1p-1h contributions due to the $(1d_{3/2}, 1p_{1/2}^{-1})$ and $(1d_{5/2}, 1p_{1/2}^{-1})$ single particle-hole contributions, respectively.

by a factor 0.93 in order to obtain better agreement with the data. This same normalization was used to calculate the angular distribution at $E_p = 49.69$ MeV also shown in the figure. The values obtained for the GDR built on this cluster are $E_\gamma = 20.7$ MeV and $\Gamma_\gamma = 3$ MeV.

The experimental analyzing powers for the γ "$_{13}$" cluster of states is shown in Fig. 5(c). No theoretical analyzing powers were calculated for this cluster since it is impossible to obtain the relative strength of the three states from the unresolved structure. However, shown in the figure are analyzing powers calculated by the program HIKARI, for pure $(1d_{5/2}, 1p_{1/2}^{-1})$ and $(1d_{3/2}, 1p_{1/2}^{-1})$ states in order to show the general trend of the calculations. The approximate agreement between the measured values and the $(1d_{5/2}, 1p_{1/2}^{-1})$ configuration calculation may indicate this configuration is, in fact, the dominant one for the cluster.

V. CONCLUSIONS

When the $\theta_\gamma = 60°$ energy dependence of the differential cross sections populating the excited states studied are plotted as a function of γ-ray energy as in Fig. 6, all the yields show evidence for giant resonances built on the various excited states and these GDR's peak at approximately ($E_\gamma = 22.441$ MeV) the same γ-ray energy (± 2 MeV) above the states which they are built as does the ground state GDR. Such excitations were predicted by Brink[30] and Axel[31] and have been verified in other experiments.[2,3,4,25,26,32,33] Giant dipole resonances have also been observed by analyzing gamma-ray energy distributions in heavy-ion fusion reactions,[34] and most recently giant resonances built on isobaric analog states were observed in pion double-charge exchange experiments.[35] At this point the Brink-Axel hypothesis on the existence of giant resonances built on excited states appears to be very well confirmed.

Both the phenomenological and the relativistic DSD model calculations presented here give reasonable fits to the energy dependence and the angular distributions of the differential cross sections. The phenomenological DSD calculation gives a better fit to the analyzing power data than the relativistic calculations. A sizable set of (p,γ) analyzing power data has by now been gathered. These data appear to present a substantial challenge for developing new theoretical approaches to the details of radiative capture reactions in the energy range studied here.

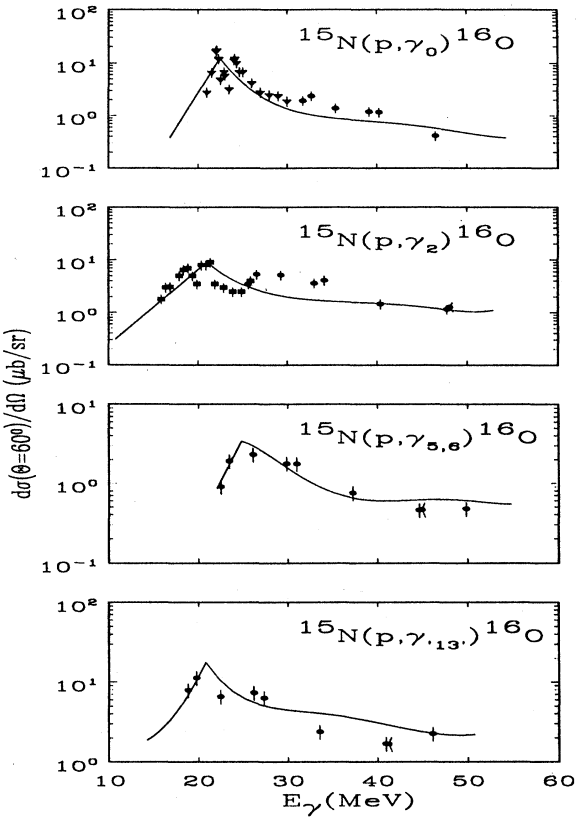

FIG. 6. Comparison of energy dependencies of the differential cross sections for the states of interest in ^{16}O vs E_γ, with the phenomenological DSD calculation described earlier; GDR's built on these states are clearly indicated.

ACKNOWLEDGMENTS

We wish to thank H. W. Dyke and R. L. Johnson for their assistance with the OMEGA gamma-ray spectrometers. This work was supported in part by the National Science Foundation under Grant PHY-8504733.

*Present address: University of New Hampshire, Durham, NH 03824.

†Present address: Naval Coastal Systems Center, Panama City, FL 32407.

‡Present address: Department of Physics, Clark University, Worcester, MA 01610.

[1] M. A. Kovash, Ph.D. thesis, Ohio State University, 1978.

[2] H. Weller, H. Hasan, S. Manglos, G. Mitev, N. R. Roberson, S. L. Blatt, H. J. Hausman, R. G. Seyler, R. N. Boyd, T. R. Donoghue, M. A. Kovash, A. Bacher, and C. Foster, Phys. Rev. C **25**, 2921 (1982); S. L. Blatt, M. A. Kovash, H. J. Hausman, T. R. Donoghue, R. N. Boyd, A. D. Bacher, and C. C. Foster, *Giant Multipole Resonances* (Harwood, Chew, Switzerland, 1980), p. 435; S. L. Blatt, in *Proceedings of the International Conference on Nuclear Structure, Amsterdam, 1987*, (Scholar's Press, Amsterdam, 1987), p. 86.

[3] M. Anghinolfi, P. Corvisiero, G. Ricco, M. Sanzone, M. Taiuti, and A. Zucchiatti, Phys. Rev. C **28**, 1005 (1983).

[4] D. Dowell, G. Feldman, K. Snover, A. Sandorfi, and M. Collins, Phys. Rev. Lett. **50**, 1191 (1983).

[5]H. J. Hausman, S. L. Blatt, T. R. Donoghue, J. D. Kalen, W. Kim, D. G. Marchlenski, T. W. Rackers, P. Schmalbrock, M. A. Kovash, and A. Bacher, Phys. Rev. C **37**, 503 (1988).
[6]G. E. Brown, Nucl. Phys. **57**, 339 (1964).
[7]A. Lushnikov and D. Zaretsky, Nucl. Phys. **66**, 35 (1965).
[8]C. Clement, A. Lane, and J. Rook, Nucl. Phys. **66**, 293 (1965).
[9]M. Potokar, A. Likar, F. Cvelbar, M. Budnar, and H. Hodgson, Nucl. Phys. **A213**, 525 (1973).
[10]M. Potokar, Phys. Lett. **92B**, 1 (1980).
[11]H. Kitazawa, private communication. Code provided by H. Weller, Duke University.
[12]M. Wright, H. Kitazawa, N. Roberson, H. Weller, M. Jensen, and D. Tilley, Phys. Rev. C **31**, 1125 (1985).
[13]W. R. Dodge, E. Hayward, R. G. Leicht, M. McCord, and R. Starr, Phys. Rev. C **28**, 8 (1983).
[14]G. Perrin, D. Lebrun, J. Chauvin, P. Martin, P. DeSantignon, D. Eppel, H. V. Geramb, H. L. Yadav, and V. A. Madsen, Phys. Lett. **66B**, 55 (1977).
[15]S. Hanna, H. Glavish, R. Avida, J. Calarco, E. Kuhlmann, and R. LaCanna, Phys. Rev. Lett. **32**, 114 (1974).
[16]A. Sandorfi, M. Collins, D. Millener, A. Nathan, and S. LeBrun, Phys. Rev. Lett. **46**, 884 (1981).
[17]B. Watson, P. Singh, and R. Segel, Phys. Rev. **182**, 977 (1969).
[18]C. J. Horowitz and B. D. Serot, Nucl. Phys. **A368**, 503 (1981).
[19]J. R. Shepard, J. A. McNeil, and S. L. Wallace, Phys. Rev. Lett. **50**, 1443 (1983).
[20]B. C. Clark, S. Hama, and R. L. Mercer, in *Interactions Between Medium Energy Nucleons and Nuclei (Indiana Cyclotron Facility, Bloomington, Indiana),* Proceedings of the Workshop on the Interactions Between Medium Energy Nucleon in Nuclei, AIP Conf. Proc. No. 97, edited by Hans-Otto Meyer (AIP, New York, 1983).
[21]J. P. McDermott and J. Shepard, *Proceedings of the Sixth International Capture Gamma-Ray Symposium, Belgium, 1987,* edited by K. Abrahams and P. Van Assche (IOP Publishing, Bristol, 1988), p. 724; J. P. McDermott, Ph.D. thesis, University of Colorado, 1986; J. P. McDermott, E. Rost, J. R. Shepard, and C. Y. Cheung, Phys. Rev. Lett. **61**, 814 (1988).
[22]J. Baglin and M. Thompson, Nucl. Phys. **A138**, 73 (1969).
[23]D. Findlay and R. Owens, Nucl. Phys. **A279**, 385 (1977).
[24]E. Earl and N. Tanner, Nucl. Phys. **A95**, 241 (1967).
[25]S. Chew, J. Lowe, and J. Nelson, Nucl. Phys. **A281**, 451 (1977).
[26]D. P. Balamuth, K. D. Braun, T. Chapuran, and C. M. Laymos, Phys. Rev. C **36**, 2235 (1987).
[27]P. Corvisiero, M. Taiuti, A. Zucchiatti, and M. Anghinolfi, Nucl. Instrum. Methods **185**, 291 (1981).
[28]M. Taiuti, M. Anghinolfi, P. Corvisiero, G. Ricco, and A. Zuchiatti, Nucl. Instrum. Methods **211**, 135 (1983).
[29]H. Fulbright, J. Robbins, M. Blann, D. Fleming, and H. Plendl, Phys. Rev. **184**, 1068 (1969).
[30]D. Brink, Ph.D. thesis, Oxford University, 1955.
[31]P. Axel, Phys. Rev. **126**, 671 (1962).
[32]M. Anghinolfi, P. Corvisiero, G. Ricco, M. Taiuti, and A. Zucchiatti, Nucl. Phys. **A399**, 66 (1983).
[33]S. L. Blatt, Los Alamos National Laboratory Report No. LA-8303-C, 1980, p. 90.
[34]D. R. Chakrabarty, S. Sen, M. Thoennessen, N. Alamanos, P. Paul, R. Schieker, J. Stachel, and J. J. Gaardhoje, Phys. Rev. C **36**, 1986 (1987).
[35]S. Mordechai, N. Auerbach, G. R. Burleson, K. S. Dhuga, M. Dwyer, J. A. Faucett, H. T. Fortune, R. Gilman, S. J. Greene, C. Laymon, C. Fred Moore, C. L. Morris, D. S. Oakley, M.